Antiferromagnetism in $CeAu_2Si_2$- and $CeAg_2Si_2$-based Kondo-lattice systems

1994 J. Phys.: Condens. Matter 6 8585

(http://iopscience.iop.org/0953-8984/6/41/020)

J. Phys.: Condens. Matter 6 (1994) 8585–8598. Printed in the UK

Antiferromagnetism in $CeAu_2Si_2$- and $CeAg_2Si_2$-based Kondo-lattice systems

C S Garde and J Ray

Low Temperature Physics Group, Tata Institute of Fundamental Research, Homi Bhabha Road, Colaba, Bombay–400 005, India

Received 5 April 1994, in final form 28 June 1994

Abstract. We report the electrical resistivity ρ, thermopower S and thermal conductivity λ of $Ce_{1-x}La_xAu_2Si_2$, $Ce_{1-y}Y_yAu_2Si_2$, $Ce_{1-x}La_xAg_2Si_2$ and $Ce_{1-y}Y_yAg_2Si_2$ ($0 \leqslant x, y \leqslant 1$) systems. The ρ curves show a sudden change in slope at the antiferromagnetic ordering temperature T_N^ρ. In the $CeAu_2Si_2$-based alloys, the T_N depression, due to the dilution of Ce atoms by La or Y, is accounted for solely by the weakening of the inter-site interaction temperature scale T_{RKKY}. On the other hand, in the $CeAg_2Si_2$-based alloys, apart from T_{RKKY}, the single-ion Kondo temperature T_K also plays an important role in determining the nature of the T_N variation. The ρ and λ behaviours, at both low and high temperatures, show clear evidence for the Kondo effect in the presence of crystal fields.

1. Introduction

The magnetic behaviour of Ce-based Kondo-lattice (KL) compounds has usually been found to be governed by two important temperature scales. The first one is the single-ion Kondo temperature $T_K \propto \exp(-1/NJ)$, and the second one is the inter-site interaction temperature $T_{RKKY} \propto NJ^2$. Here J is the magnetic exchange integral between the 4f electron of the Ce ion and the surrounding conduction electrons, and N is the density of states (DOS) at the Fermi energy E_F. The strength of J also depends on two effects. The first one is referred to as the 'volume effect', where J depends on the unit-cell volume of the system. The smaller this unit-cell volume, the greater is the 4f conduction electron overlap giving rise to increase in the magnitude of J. The second one is referred to as the 'electronic effect', where J depends on the DOS at E_F. These electronic effects arise due to the electrons that give rise to narrow bands near E_F. Several investigations [1–3] on Ce-based systems attempted to understand the precise role of J. Different ground states, varying from the heavy-fermion (HF) antiferromagnetic (AF) ground state to a mixed-valent (MV) one, due to the competing influences of T_K and T_{RKKY}, have been observed. For example, in the $Ce(Cu_{1-x}Ni_x)_2Si_2$ alloy series, for $x > x_c$ ($x_c \simeq 0.4$), a cross-over from HF to MV behaviour has been observed. This cross-over has been identified [4] with the anomalous increase (in contrast to the usual linear variation) of the Ce–X (X = Ni or Cu) distance d with x giving rise to a decrease in the value of J at x_c. In $Ce(Ru_{1-x}Rh_x)_2Si_2$, a magnetically ordered phase [5] has been found to develop, from the HF behaviour, when Ru is replaced by non-isovalent Rh. As x is increased (from $x = 0$), T_N first increases and then decreases and goes to zero at $x = 0.3$. Such a behaviour has been attributed to competition between the volume and the electronic effects. In view of this interest in recent years, we have studied and compared two magnetically ordered CeM_2Si_2 (M = Au, Ag) compounds. Though Ag

0953-8984/94/418585+14$19.50

and Au are isovalent, Au has extra 5d electrons and hence, apart from the volume effects, the electronic effects also could contribute to J in these two compounds. Such a situation has also been studied recently even in binary compounds like CeCd and CeZn, where Cd and Zn are both isovalent. Our transport measurements are thus aimed at examining the complex role played by the volume as well as the electronic effects for the M = Au, Ag systems.

$CeAu_2Si_2$ and $CeAg_2Si_2$ both exhibit [6–9] an antiferromagnetic (AF) order below T_N = 10 and 9.4 K, respectively. In the AF state of $CeAu_2Si_2$, the value [7] of the moment on the Ce ions is about 1.29 μ_B, arising from the crystal-field (CF) ground state [10]. In $CeAg_2Si_2$, the Ce moment value [7] is about 0.73–0.93 μ_B. This reduction in the moment value from the expected value of 1.3 μ_B, for doublet CF ground state, is attributed [11] to the presence of a Kondo effect in the ordered state at low temperatures. The value of T_K = 1.7 and 5 K for $CeAu_2Si_2$ and $CeAg_2Si_2$, respectively, has been deduced from neutron studies [11, 12].

In order to understand the complex magnetic behaviour of the CeM_2Si_2 (M = Ag, Au) compounds, we have investigated the $Ce_{1-x}La_xM_2Si_2$ and $Ce_{1-y}Y_yM_2Si_2$ alloy series. The variation of the parent CeM_2Si_2 compound by controlling x and y would provide a means of altering the value of J through both the volume and the electronic effects. Thus our alloy series would enable one to study the relative strength of T_K and T_{RKKY} and subsequently that of T_N by this variation of J.

2. Sample preparation and x-ray analysis

All the alloys were prepared in an arc furnace by repeated melting in flowing argon. They were found to show a single phase of the $ThCr_2Si_2$ orthorhombic structure type, using an x-ray diffractometer (JEOL, Japan). The values (tables 1 and 2) of the lattice parameters a and c of both $CeAu_2Si_2$ and $CeAg_2Si_2$ are found to be close to values reported earlier [6]. For $Ce_{1-x}La_xAu_2Si_2$, with the variation of x from 0 to 1, c was found (table 1) to remain constant, whereas a was found to increase by 0.5% over the same concentration range. As a consequence, the unit-cell volume V increased (table 1) by 1%. For $Ce_{1-y}Y_yAu_2Si_2$, both a and c decreased with increase of y. Consequently, V decreased by about 3.9%. Similarly for $Ce_{1-x}La_xAg_2Si_2$, c was found (table 2) to be constant with increasing x, whereas a increased by 1%. Consequently, V increased by 2%. For $Ce_{1-y}Y_yAg_2Si_2$, both a and c decreased and therefore V decreased by 2.9% as y was increased from 0 to 1. Thus, with increasing substitution of La ions (of ionic radius larger than Ce), the cell size gradually expanded, whereas by substitution of Y ions (of ionic radius smaller than Ce) it was compressed with respect to the parent lattice (y = 0). Therefore, chemical pressure effects were clearly seen in these samples. Further, for $CeAg_2Si_2$, the value of c/a is found to be 2.5, which is the largest amongst the compounds [12] of the CeM_2Si_2 (M = Au, Pd, Cu, Ru) series. Thus, the Ce–X distance d is the largest for $CeAg_2Si_2$ compared to that for other compounds of the above series.

3. Results

3.1. $CeAu_2Si_2$-based systems

3.1.1. Antiferromagnetic behaviour. The ρ curve of $CeAu_2Si_2$ exhibits (figure 1) a sudden change in the slope ($\partial\rho/\partial T$) at T_N^ρ = 9.4 K (table 3). This value of T_N^ρ is found to be

Table 1. Lattice constants a and c and the unit-cell volume V for $(Ce_{1-x}La_x)Au_2Si_2$ and $(Ce_{1-y}Y_y)Au_2Si_2$ systems.

System	a (Å)	c (Å)	V (Å^3)
$Ce_{1-x}La_xAu_2Si_2$			
$x = 0$	4.318 ± 0.001	10.223 ± 0.003	190.6 ± 0.1
0.05	4.320 ± 0.003	10.215 ± 0.012	190.6 ± 0.1
0.15	4.321 ± 0.006	10.219 ± 0.010	190.8 ± 0.1
0.40	4.326 ± 0.005	10.222 ± 0.012	191.3 ± 0.1
0.70	4.333 ± 0.006	10.220 ± 0.009	191.9 ± 0.1
1.00	4.339 ± 0.003	10.225 ± 0.008	192.5 ± 0.1
$Ce_{1-y}Y_yAu_2Si_2$			
$y = 0.05$	4.317 ± 0.001	10.223 ± 0.002	190.5 ± 0.1
0.15	4.315 ± 0.004	10.226 ± 0.011	190.4 ± 0.1
0.40	4.296 ± 0.005	10.204 ± 0.013	188.3 ± 0.1
1.00	4.240 ± 0.004	10.181 ± 0.009	183.0 ± 0.1

Table 2. Lattice constants a and c and the unit-cell volume V for $(Ce_{1-x}La_x)Ag_2Si_2$ and $(Ce_{1-y}Y_y)Ag_2Si_2$ systems.

System	a (Å)	c (Å)	V (Å^3)
$Ce_{1-x}La_xAg_2Si_2$			
$x = 0$	4.285 ± 0.005	10.552 ± 0.016	193.7 ± 0.1
0.05	4.294 ± 0.015	10.553 ± 0.017	194.6 ± 0.1
0.40	4.307 ± 0.047	10.547 ± 0.014	195.6 ± 0.1
0.70	4.312 ± 0.046	10.543 ± 0.014	196.0 ± 0.1
1.00	4.328 ± 0.010	10.540 ± 0.020	197.4 ± 0.1
$Ce_{1-y}Y_yAg_2Si_2$			
$y = 0.05$	4.280 ± 0.006	10.549 ± 0.020	193.2 ± 0.1
0.40	4.256 ± 0.068	10.515 ± 0.104	190.5 ± 0.1
0.70	4.247 ± 0.021	10.502 ± 0.044	189.4 ± 0.1
1.00	4.231 ± 0.070	10.487 ± 0.036	187.7 ± 0.1

quite close to that of T_N found from the χ and neutron studies [7, 8]. With both La and Y substitutions, T_N^ρ is found (figure 2) to decrease, indicating the weakening of the AF order. The value (table 3) of T_N^ρ is found to decrease almost linearly (figure 2) at the same rate with increase of either x or y. Further, on extrapolating to higher concentrations ($x, y > 0.7$), we find $T_N^\rho \to 0$ for $x, y \to 1$. Such a linear variation of T_N, with increasing x or y, could be accounted for solely by the weakening of the Ruderman–Kittel–Kasuya–Yosida (RKKY) interaction strength T_{RKKY} between the Ce ions. The influence of the Kondo effect on the AF ordering temperature T_N^ρ is thus negligible. This also supports the earlier estimate [11] of $T_K \sim 1.7$ K, which is much lower than T_N. It is known [13] that $T_{RKKY} \propto CJ^2$, where $C(= 1 - x)$ is the concentration of the Ce ions. Therefore we find that $T_{RKKY} \to 0$ as $C \to 0 (x, y \to 1)$. This shows that the variation of T_N arises due to changes in C alone. Any change in the value of J, with the variation of C, is thus considered negligible. This conclusion is also supported [9] by the observation of a negligible variation of T_N in $CeAu_2Si_2$ with external pressure. Even though the lattice was compressed, J remained unaffected, thereby keeping the value of T_N constant. Further, for $CeAu_2Si_2$, we have $T_K/T_N < 1$. This would correspond to a point located (figure 3) on the left-hand side of the peak of Doniach's $T_N(J)$ magnetic phase diagram.

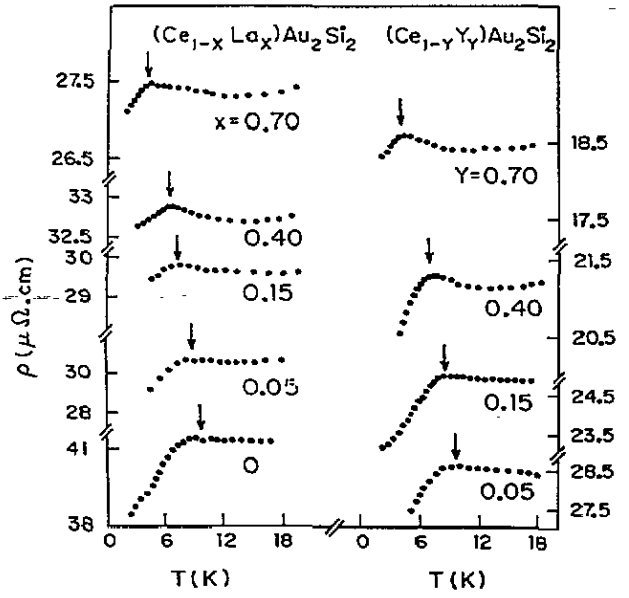

Figure 1. Low-temperature ρ versus T curves for $(Ce_{1-x}La_x)Au_2Si_2$ and $(Ce_{1-y}Y_y)Au_2Si_2$ systems. The arrows indicate the temperatures where the magnetic transitions occur.

Table 3. Values of the various characteristic temperatures for CeM_2Si_2-based systems (M = Au, Ag).

System	T_N^ρ (K)	T_{min}^ρ (K)	T_{max}^ρ (K)	T_0^S (K)	T_{min}^S (K)	T_{max}^S (K)	T_{min}^W (K)	T_{max}^W (K)
$Ce_{1-x}La_xAu_2Si_2$								
$x = 0$	9.4	25	100	—	30	—	24	120
0.05	8.8	25	100	—	20	—	24	110
0.15	7.8	25	100	—	20	—	20	115
0.4	6.4	20	100	—	20	—	16	125
0.7	4.0	—	—	—	15	—	—	—
$Ce_{1-y}Y_yAu_2Si_2$								
$y = 0.05$	9.0	25	100	—	30	—	20	120
0.15	8.0	25	100	—	30	—	18	125
0.4	6.6	22	100	—	30	—	—	—
0.7	4.0	—	—	—	30	—	—	—
$Ce_{1-x}La_xAg_2Si_2$								
$x = 0$	7.3	23	100	4.0	20	70	23	120
0.05	7.1	19	100	3.8	20	65	23	100
0.4	4.3	16	100	—	20	—	23	110
0.7	2.7	13	100	—	25	—	—	—
$Ce_{1-y}Y_yAg_2Si_2$								
$y = 0.05$	7.6	22	100	4.1	30	70	20	120
0.4	6.0	30	100	—	30	80	18	95
0.7	4.1	—	—	—	35	90	—	—

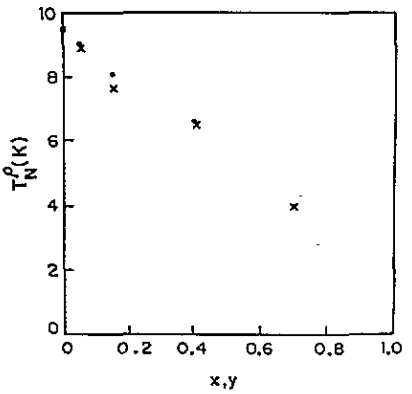

Figure 2. Variation of T_N^ρ with x (×) and y (○) in $(Ce_{1-x}La_x)Au_2Si_2$ and $(Ce_{1-y}Y_y)Au_2Si_2$ systems, respectively.

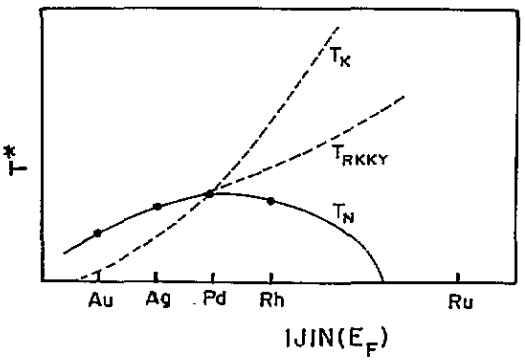

Figure 3. Doniach's magnetic phase diagram showing the schematic variation of the characteristic temperature scales (T_K, T_{RKKY}, T_N) versus $|J|N(E_F)$. The symbols M = Au, Ag, Pd, Rh, Ru on the x axis denote the relative position of the various CeM_2Si_2 compounds on this diagram.

3.1.2. Magnetic resistivity and Kondo behaviour. The magnetic behaviour of these compounds has been further analysed by calculating the magnetic contribution ρ_m. This contribution is obtained by subtracting the resistivity of non-magnetic $LaAu_2Si_2$ and YAu_2Si_2 from that of the $Ce_{1-x}La_xAu_2Si_2$ and $Ce_{1-y}Y_yAu_2Si_2$ systems, respectively. The ρ_m curve for all the systems exhibits a logarithmic temperature dependence (figure 4) for $T_N < T < 20$ K and 150 K $< T <$ 300 K, respectively. This logarithmic behaviour (with negative slope) is a characteristic signature [14] of the Kondo process in the presence of CF effects. The low-temperature logarithmic behaviour (figure 4) arises due to Kondo scattering from the ground state of the CF split levels of the Ce ion. On the other hand, the high-temperature one corresponds to the Kondo scattering from all the populated CF levels. The calculated value of the ratio of the slopes (of the straight-line portions of the low- and high-temperature regimes (figure 4) of the ρ_m curve) Q turns out to have a value of 0.280. This value of Q is somewhat higher than the theoretically expected value of 0.086 for a doublet CF ground state. Such departures (of the experimentally observed values from the theoretically predicted ones) have also been observed [14, 15] for $CeAl_2$- and CePdSn-based systems. This has been attributed [15] to a weak Kondo process at high temperatures.

Further, the ρ_m curve (figure 4) exhibits a minimum and a maximum at $T_{min}^\rho \sim 25$ K and $T_{max}^\rho \sim 100$ K, respectively. The value of T_{max}^ρ has been theoretically predicted [14] to be approximately equal to the overall CF splitting Δ_{CF}. Our measured value of $T_{max}^\rho \sim 100$ K, for $CeAu_2Si_2$, is smaller than $\Delta_{CF} \sim 220$ K estimated from neutron studies [10]. Both ρ_{min} and ρ_{max} are not discernible for the $x, y = 0.7$ alloys. Further, the magnitude of ρ_m (~ 10 $\mu\Omega$ cm), for $CeAu_2Si_2$-based systems, is found to be comparable to that observed [16, 17] for the $CeCu_2$ and $CeCu_5$ compounds.

3.1.3. Thermopower behaviour. We now examine the S behaviour. For the pure $CeAu_2Si_2$ ($x = 0$) compound, the S curve exhibits (figure 5) a negative minimum S_{min}, at $T_{min}^S \sim 30$ K (table 3), and then crosses over to a positive value for $T > 60$ K. No feature is observed at T_N^ρ, indicating that S has no characteristic signature to denote the onset of magnetic ordering effects. The occurrence of S_{min} is also a usual feature and is observed [13, 18, 19] in many KL systems like $CeAl_3$, $CeCu_2Si_2$ and $CePd_2Si_2$. This S_{min} has also been naively attributed

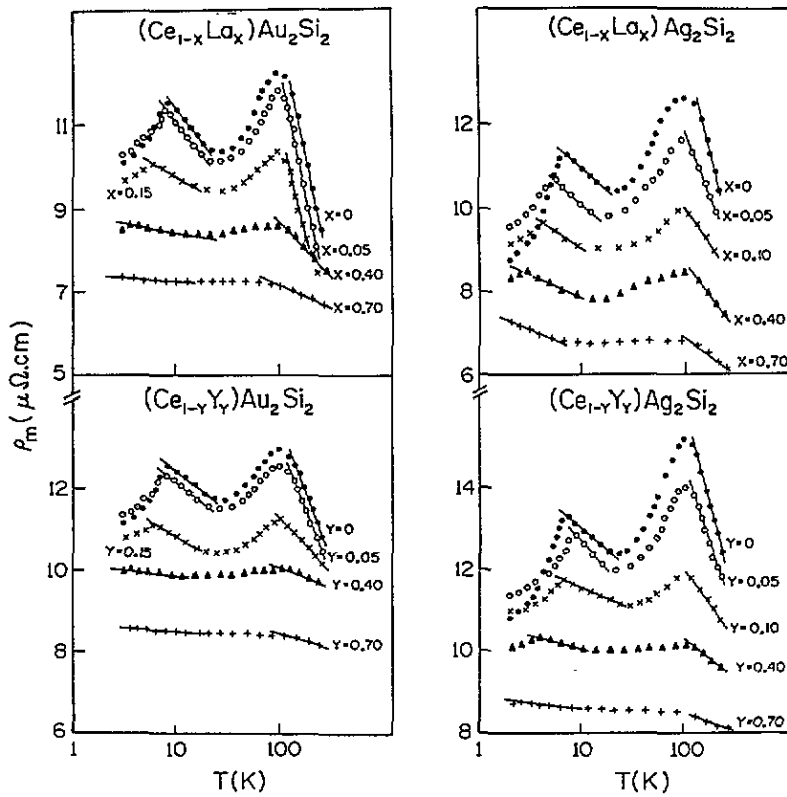

Figure 4. Curves of ρ_m versus T for the $(Ce_{1-x}La_x)Au_2Si_2$, $(Ce_{1-y}Y_y)Au_2Si_2$, $(Ce_{1-x}La_x)Ag_2Si_2$ and $(Ce_{1-y}Y_y)Ag_2Si_2$ systems. Temperature is plotted on logarithmic scale. The straight-line portions indicate the logarithmic variation of ρ_m with temperature.

[18, 20] to single-ion Kondo effects. T^S_{min} is found to decrease (table 3) with increase in x. For $x = 0.7$, T^S_{min} drops to 15 K, whereas with Y substitution, T^S_{min} is found to remain constant (table 3) up to $y = 0.7$.

At higher temperatures ($T > 60$ K), the S curves for $x \leqslant 0.7$ do not exhibit the usual [16, 20] broad positive maximum seen in many KL compounds due to the combined effect of Kondo scattering from the excited CF states and the non-magnetic terms. The value ($\simeq 2$ μV K^{-1}) of S, for $CeAu_2Si_2$, is of a magnitude comparable (figure 5) to the non-magnetic compounds like $LaAu_2Si_2$ and YAu_2Si_2. In contrast, the magnetic KL compounds usually have large values (~ 50 μV K^{-1}) due to anisotropic scattering mechanisms. In these systems, the small value of S could be related to the small value of ρ_m as observed [16, 17] also in other KL systems like $CeCu_2$ and $CeCu_5$. This indicates that the magnetic contribution in $CeAu_2Si_2$-based alloys is quite small. We note that definite signatures regarding the Kondo behaviour are not presently known, unlike those which manifest in the ρ_m data.

3.1.4. Thermal conductivity and Kondo behaviour. The λ behaviour of these systems is analysed now. The total contribution to λ is expressed [21, 22] as $\lambda = \lambda_e + \lambda_l$, where λ_e and λ_l are the electronic and lattice contributions, respectively. Assuming Matthiessen's rule to be valid, λ_e can be expressed [21] as follows:

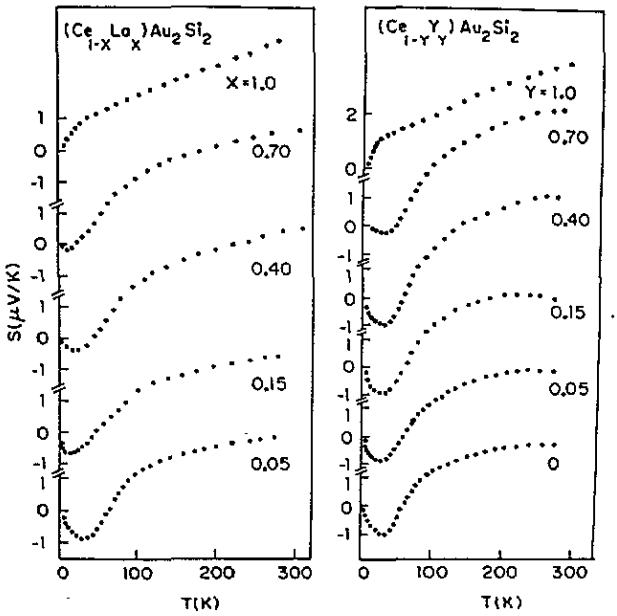

Figure 5. Curves of S versus T for the $(Ce_{1-x}La_x)Au_2Si_2$ and $(Ce_{1-y}Y_y)Au_2Si_2$ systems.

$$1/\lambda_e = W_e = W_{e,0} + W_{e,ph} + W_{e,m} \tag{1}$$

where W_e is the electronic contribution to the thermal resistivity (inverse of the thermal conductivity) and $W_{e,0}$, $W_{e,ph}$ and $W_{e,m}$ represent the thermal resistivity arising due to electron scattering from static imperfections, phonons and magnetic moments, respectively. We assume that (i) $\lambda_e \gg \lambda_l$ and (ii) the non-magnetic electronic contribution $(W_{e,0} + W_{e,ph})$ is the same for the non-magnetic (pure La and Y compounds) and the Ce-based ones. Under these conditions, $W_{e,m}$ becomes equal to the difference ΔW between the thermal resistivities of the Ce-based and the pure non-magnetic (La and Y) alloys.

Similar to the ρ_m curves, the ΔWT ones also exhibit (figure 6) a logarithmic behaviour both in the low-temperature (10–20 K) as well as in the high-temperature (150–300 K) ranges. These curves exhibit a minimum and a maximum at $T^W_{min} \sim 24$ K and $T^W_{max} \sim 120$ K. The general shapes are also quite similar to those observed in the ρ_m curves (figure 4), which arise [21, 22] due to the Kondo scattering process in the presence of CF effects.

This similarity, between the ρ_m and ΔWT data, can be understood by considering the Weidemann–Franz (WF) law. This law relates λ and ρ through the relation $\lambda\rho/T = L$. Thus $W(= 1/\lambda) \propto \rho$ and therefore $(\Delta WT) \propto \rho_m$. In the free-electron picture, L is a temperature-independent quantity $L_0 = 2.45 \times 10^{-8}$ W Ω K^{-2}. L_0 is usually called the Sommerfeld value or the Lorenz number. In general, when the free-electron approach is not valid, the Lorenz number, designated as $L(T)$, is temperature-dependent and could be widely different from L_0. In our systems, the value of $L(T)$ (calculated using $L = \lambda\rho/T$) at 10 K is found (figure 7) to have an almost fourfold variation from L_0. The value of L/L_0 is close to 1 only for $T > 75$ K. This clearly indicates that the WF law holds true at high temperatures but is not valid at low temperatures ($T < 20$ K). One reason for the large values of L/L_0 at low temperatures is that the assumption $\lambda_e \gg \lambda_l$ may not be valid. To check this point, the λ_l contribution has been estimated [22] at low temperatures ($T < 60$ K)

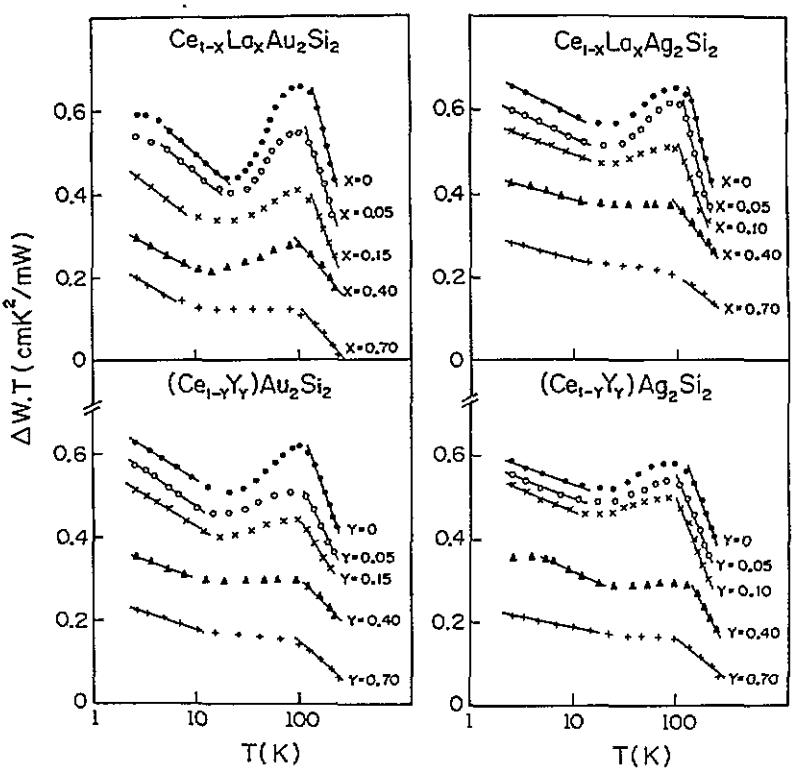

Figure 6. ΔWT versus T curves for the $(Ce_{1-x}La_x)Au_2Si_2$, $(Ce_{1-y}Y_y)Au_2Si_2$, $(Ce_{1-x}La_x)Ag_2Si_2$ and $(Ce_{1-y}Y_y)Ag_2Si_2$ systems. Temperature is plotted on logarithmic scale. The straight-line portions indicate the logarithmic variation of ρ_m with temperature.

by fitting (figure 8) the λ behaviour of the non-magnetic (La- and Y-based) compounds to the following equation [22]:

$$\lambda = \lambda_c + \lambda_l = (A/T + BT^2)^{-1} + DT^2 \tag{2}$$

where A, B and D are constants. The values of the constants are tabulated in table 4. At $T = 10$ K, for the non-magnetic M = Au compounds, $\lambda_l (= DT^2)$ is found (table 4) to be as much as 4–5% of the total λ. Further, for the magnetic systems ($x, y \neq 1$), λ_l would account for an even larger fraction of λ because λ_c in these systems would get reduced, compared to non-magnetic compounds, owing to the presence of magnetic scattering (see equation (1)). This is reflected in the larger values of (i) λ (figure 8) for the non-magnetic (La and Y) compounds and (ii) L/L_0 (figure 7) for the magnetic compounds. The ΔWT behaviour does not exhibit (figure 6) any feature at T_N, probably due to deviations from the WF law in this temperature range. However, at higher temperatures ($T > T_N$), the characteristic features for the Kondo scattering in the presence of CF effects are clearly observed in the ΔWT behaviour.

3.2. *$CeAg_2Si_2$-based systems*

3.2.1. Antiferromagnetic behaviour. The ρ curve of $CeAg_2Si_2$ exhibits (figure 9) a maximum at the AF ordering temperature $T_N^\rho = 7.3$ K (table 3). The value of T_N^ρ is smaller than the

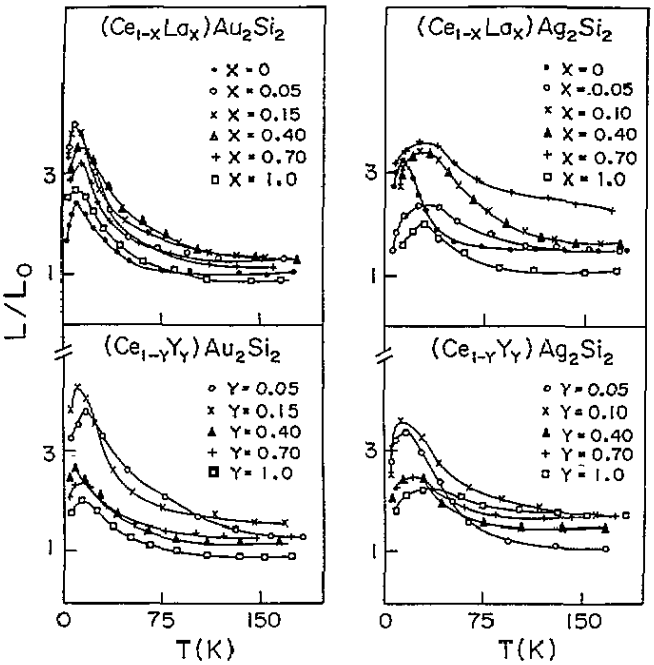

Figure 7. L/L_0 versus T curves for the $(Ce_{1-x}La_x)Au_2Si_2$, $(Ce_{1-y}Y_y)Au_2Si_2$, $(Ce_{1-x}La_x)Ag_2Si_2$ and $(Ce_{1-y}Y_y)Ag_2Si_2$ systems. Lines passing through the points are hand drawn to guide the eye.

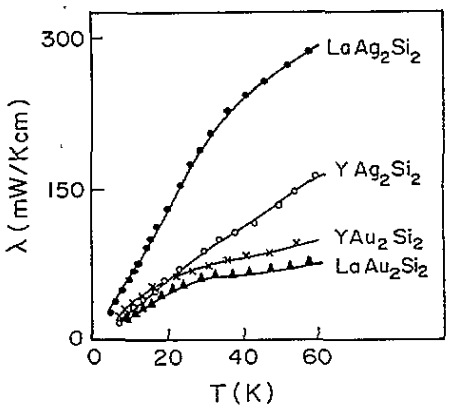

Figure 8. Low-temperature λ versus T curves for $LaAu_2Si_2$, YAu_2Si_2, $LaAg_2Si_2$ and YAg_2Si_2. The full curves are fitted curves obtained by using equation (2).

Table 4. Values of the parameters obtained, for the non-magnetic compounds, by fitting (using equation (2)) the λ data in the temperature range 2–60 K.

Compound	A (cm K^2 mW^{-1})	B (cm mW^{-1} K^{-1})	D (mW K^{-3} cm^{-1})	λ_l/λ (T = 10 K) (%)
$LaAu_2Si_2$	0.3682	0.679×10^{-5}	0.111×10^{-1}	4.0
YAu_2Si_2	0.3219	0.593×10^{-5}	0.154×10^{-1}	4.8
$LaAg_2Si_2$	0.3899	0.252×10^{-5}	0.258×10^{-1}	9.2
YAg_2Si_2	0.1594	0.606×10^{-5}	0.243×10^{-1}	3.7

value of $T_N = 9.5$ K estimated from earlier χ and neutron studies [6–8, 23]. For the $Ce_{1-x}La_xAg_2Si_2$ alloys, T_N^ρ is found (table 3) to decrease (figures 9 and 10) with increase in x. This decrease (figure 10) is almost linear with increase in x. Further, we find $T_N^\rho \to 0$ as $x \to 1$, which can again be interpreted, as discussed for the M = Au case, on the basis of dilution of Ce ions by La ions. On the other hand, for the $Ce_{1-y}Y_yAg_2Si_2$ alloys, T_N is found (figure 10) to increase initially up to $y = 0.05$, over that for the pure $CeAg_2Si_2$ compound ($y = 0$). Subsequently, T_N^ρ decreases in the usual manner for $y > 0.05$. We note that for the same value of $x = y$, the value (table 3) of T_N^ρ is found (figure 10) to be larger for the Y-substituted alloys than that for the La-substituted alloys. This enhancement of T_N, for the Y-substituted alloys over the La-substituted ones, indicates that the variation of T_N with y cannot be accounted for only by dilution of Ce by Y atoms. This is because, for $CeAg_2Si_2$, the addition of Y compresses the lattice leading to an increase in the value of J. The value of T_N is also sensitive to external pressure. The increase (figure 10) in the value of T_N, for small values of y ($\leqslant 0.05$), suggests that $CeAg_2Si_2$ would also be located on the left-hand side of the peak of the $T_N(J)$ diagram. Further, as $T_K \leqslant T_N$, it would be located (figure 3) closer to the peak (near $CePd_2Si_2$) than $CeAu_2Si_2$. In the case of $CePd_2Si_2$, $T_K = T_N$ [12], and this compound is therefore situated (figure 3) at the peak of the $T_N(J)$ diagram. On the other hand, $CeRh_2Si_2$, having $T_N = 36$ K [12], is located on the right-hand side of the peak because, with Y or La substitutions, the T_N gets depressed or enhanced, respectively. We note that the value of T_N results from the combined influence of T_K and T_{RKKY} and therefore the location of a particular system on the $T_N(J)$ curve (figure 3) is decided by the value of the ratio T_K/T_N and not simply by the value of T_N of the particular compound. The $T_N(J)$ model is therefore useful to study the interplay of T_K and T_{RKKY} and not for predicting the T_N value from the phase diagram. Thus, for example in the series CeM_2Si_2 (M = Au, Ag, Pd, Rh, Ru), even though $T_N(M = Au) > T_N(M = Ag)$, the M = Ag system is located (figure 3) at a point closer to the peak than the M = Au system. The M = Rh system with a much larger T_N value is also located on the same T_N curve. The M = Ru system, having a high value of $T_K = 20$ K and $T_N = 0$, corresponds to a point outside (figure 3) the $T_N(J)$ diagram.

We further note that the value of J is usually found [12] to be directly proportional to the Ce–X distance d. As mentioned earlier, the value of d, for M = Ag, is the largest amongst the CeM_2Si_2 systems. Therefore, the value of J for M = Ag should have been the smallest amongst the series. Thus, based on this criterion alone, the M = Ag compound should have been located to the left of the M = Au compound in the $T_N(J)$ phase diagram. This therefore suggests that, apart from volume effects, electronic effects (like the DOS near E_F) play an important role in determining the value of J (and hence T_K and T_{RKKY}) in the M = Ag and probably also in the other CeM_2Si_2 systems.

3.2.2. Magnetic resistivity and Kondo behaviour. The ρ_m behaviour of $CeAg_2Si_2$-based systems exhibit (figure 4) the usual logarithmic dependence, at low and high temperatures, separated by a maximum. Thus they exhibit clear signatures for Kondo scattering in the presence of CF effects. These signatures are exactly the same as those observed for the $CeAu_2Si_2$-based ones. The value of Q for $CeAg_2Si_2$ is 0.3. This value of Q is again larger than that expected [14] theoretically for a doublet CF ground state. Further, $T_{min}^\rho \sim 23$ K and $T_{max}^\rho \sim 100$ K for these systems ($x, y \leqslant 0.7$). The value (figure 4) of ρ_m, for these systems, is again of the same order of magnitude as the Au systems and comparable to that observed [16, 17] for $CeCu_2$ and $CeCu_5$ compounds.

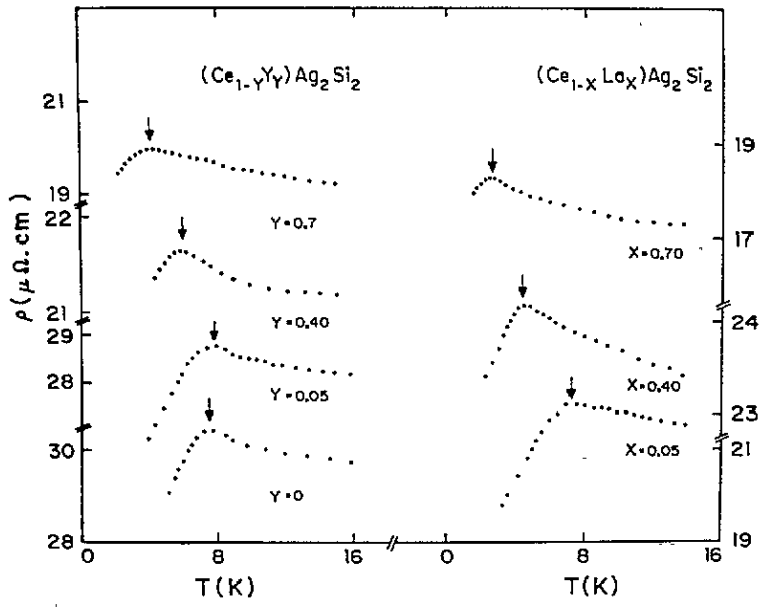

Figure 9. Low-temperature ρ versus T curves for the $(Ce_{1-x}La_x)Ag_2Si_2$ and $(Ce_{1-y}Y_y)Ag_2Si_2$ systems. The arrows indicate the temperatures where the magnetic transitions occur.

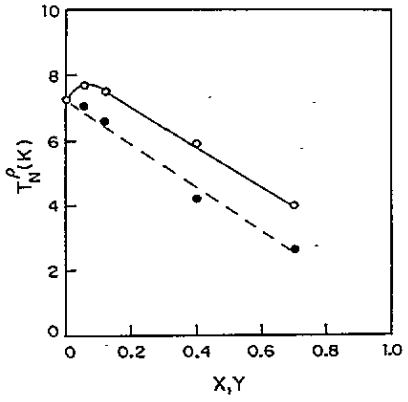

Figure 10. Variation of T_N^ρ with x (●) and y (○) in the $(Ce_{1-x}La_x)Ag_2Si_2$ and $(Ce_{1-y}Y_y)Ag_2Si_2$ systems, respectively.

3.2.3. Thermopower behaviour. The S behaviour (figure 11) of $CeAg_2Si_2$-based alloys is found to be quite anomalous. For the lower La and Y concentration ($x, y < 0.1$) systems, the curves exhibit (figure 12) a sharp positive peak at $T_0^S \simeq 4$ K. For $T > T_0^S$, the curve drops rapidly, changes sign and then goes through a negative minimum at $T_{min}^S = 20$ K. The curves again do not show any feature at T_N^ρ. The vertical arrows (figure 12) indicate the position of T_N^ρ as obtained from the ρ data. This maximum, at T_0^S (table 3), gets rapidly suppressed (figure 12) to lower temperatures for $x, y \geqslant 0.4$, even though the AF ordering persists up to $x, y = 0.7$. This suggests that the maximum is not related to magnetic ordering effects. Rather, it could arise either due to (i) the dependence of S on the variation of the DOS at the Fermi energy E_F, or (ii) coherence-derived effects as is usually observed [19] in KL systems like $CeCu_6$, $CeRu_2Si_2$ and $CeCu_2Si_2$. It is quite likely that the rapid suppression of this maximum, with increase of x or y, could then be related to the suppression of the

coherence effects caused by the breakdown of the periodicity of the Ce sublattice due to the introduction of La or Y atoms. For $T > T^S_{min}$, the curves do not become positive and develop the high-temperature maxima as observed usually in many KL systems. The usually observed behaviour, in KL systems, comprises a sharp negative minimum S_{min} at a temperature T_{min} ($T_{min} \simeq 2T_K$). For $T > T_K$, the curves cross over from negative to positive values and exhibit a broad maximum (at $T \simeq \Delta_{CF}$) due to the influence of CF states. In our systems, however, the curves (figure 11) remain negative and approach the zero value at high temperatures. This anomalous behaviour is not understood, so far, in the KL systems.

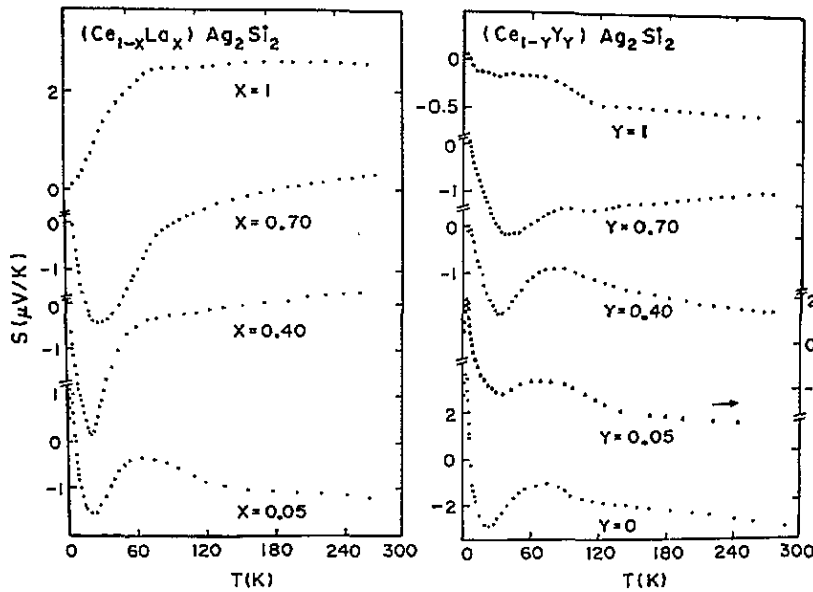

Figure 11. S versus T curves for the $(Ce_{1-x}La_x)Ag_2Si_2$ and $(Ce_{1-y}Y_y)Ag_2Si_2$ systems. The horizontal arrow indicates the appropriate y axis (on the right-hand side) pertaining to a given alloy concentration.

The low-temperature minimum S_{min}, at T^S_{min}, is related to the Kondo effect, as mentioned earlier. The value of T^S_{min} is found to remain constant (table 3) with La substitution ($x \leqslant 0.7$), whereas it is found to increase from 20 K for $y = 0$ to 35 K for $y = 0.7$. This suggests that T_K may increase with Y substitution.

At higher temperatures ($T > 40$ K), the curve for $CeAg_2Si_2$ goes through a maximum S_{max} at $T^S_{max} \simeq 70$ K (table 3). It is of interest to note that this S_{max} occurs at a negative value in contrast to the usual [13] positive S_{max} value for the Ce-based KL compounds. The overall CF splitting is given by the formula [24] $\Delta_{CF} = 3T^S_{max}$. Using the observed (table 3) value of T^S_{max}, from our studies, the calculated value is $\Delta_{CF} = 210$ K. This calculated value of Δ_{CF} is quite close to the estimated value of 190 K inferred from earlier neutron studies [10]. Further, with both La and Y substitutions, S_{max} becomes weaker and the high-temperature behaviour resembles (figure 11) that of the non-magnetic YAg_2Si_2 and $LaAg_2Si_2$ compounds, respectively.

3.2.4. Thermal conductivity and Kondo behaviour. The ΔWT behaviour (figure 6) of $CeAg_2Si_2$ and its La- and Y-substituted systems is quite similar to that observed (logarithmic

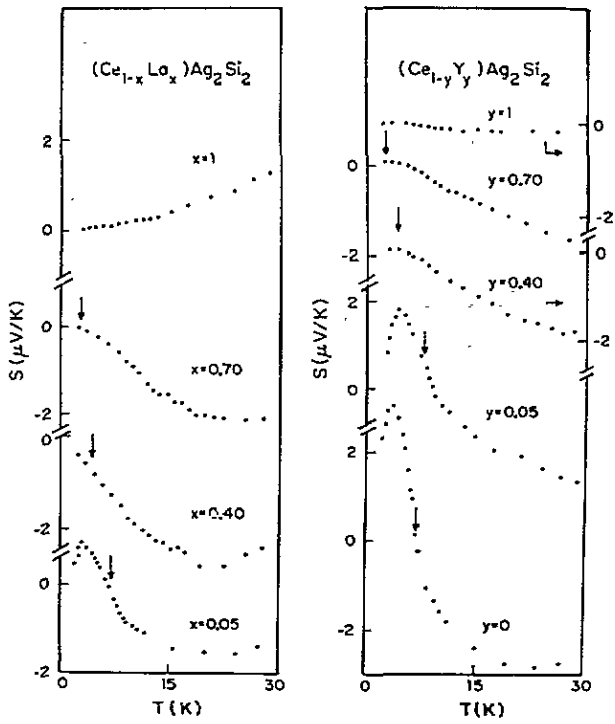

Figure 12. Low-temperature S versus T curves for the $(Ce_{1-x}La_x)Ag_2Si_2$ and $(Ce_{1-y}Y_y)Ag_2Si_2$ systems. The vertical arrows indicate the temperatures where the magnetic transitions occur. The horizontal arrows indicate the appropriate y axis (on the right-hand side) pertaining to a given alloy concentration.

behaviour at low and high temperatures) for the $CeAu_2Si_2$-based systems. The values (table 3) of T^W_{min} and T^W_{max} are ~ 23 and ~ 120 K, respectively. These curves also do not exhibit any feature at T_N. As in the case of $CeAu_2Si_2$-based systems, this absence of any feature at T_N for the $CeAg_2Si_2$-based ones could again be related to (i) the deviation from the WF law as indicated by the L/L_0 behaviour (figure 7) and (ii) the large value (table 4) of λ_l (4–9% of λ) for the pure M = Ag non-magnetic compounds.

4. Conclusions

The T_N variation, with x and y on CeM_2Si_2 (M = Au, Ag), suggests that both these compunds lie to the left of the peak of the $T_N(J)$ diagram. The low-temperature magnetic behaviour, for M = Ag, is governed not only by the volume term but also by the electronic term. The magnetic behaviour, analysed from the ρ and λ data, shows clear evidence of the Kondo effect at both low and high temperatures. For the M = Ag system, the high-temperature S_{max} is found to occur at negative values, which is unusual for the Ce-based KL systems. This behaviour is not understood in KL systems. At lower temperatures ($T < 10$ K), a sharp peak (for small values of x and y) in the S curves of the $CeAg_2Si_2$-based compounds has been observed. This could be related to coherence-derived effects.

References

[1] Shigeoka T, Uwatoko Y, Fujii H, Rebelsky L, Shapiro S M and Asai K 1990 *Phys. Rev.* B **42** 8394
[2] Continenza A and Monachesi P 1992 *Phys. Rev* B **46** 6217
[3] *Monachesi P and Continenza A 1993 Phys. Rev. B* **47** 14 622
[4] Sampathkumaran E V and Vijayaraghavan R 1986 *Phys. Rev. Lett.* **56** 2861
[5] Sekine C, Sakakibara T, Amitsuka H, Miyako Y and Goto T 1992 *J. Phys. Soc. Japan* **61** 4536
[6] Palstra T T M, Menovsky A A, Nieuwenhuys G J and Mydosh J A 1986 *J. Magn. Magn. Mater.* **54–57** 435
[7] Grier B H, Lawrence J M, Murgai V and Parks R D 1984 *Phys. Rev.* B **29** 2664
[8] Murgai V, Raaen S, Gupta L C and Parks R D 1982 *Valence Instabilities* ed P Wachter and H Boppart (Amsterdam: North-Holland) p 537
[9] Thompson J D, Parks R D and Borges H 1986 *J. Magn. Magn. Mater.* **54–57** 377
[10] Severing A, Holland-Moritz E, Raniford B D, Culverhouse S R and Frick B 1989 *Phys. Rev.* B **39** 2557
[11] Knopp G, Loidl A, Knorr K, Spille H, Steglich F and Murani A P 1988 *J. Magn. Magn. Mater.* **76/77** 420
[12] Severing A, Holland-Moritz E and Frick B 1989 *Phys. Rev.* B **39** 4164
[13] Brandt N B and Moshchalkov V V 1984 *Adv. Phys.* **33** 373
[14] Cornut B and Coqblin B 1972 *Phys. Rev.* B **5** 4541
[15] Sakurai J, Yamaguchi Y, Mibu K and Shinjo T 1990 *J. Magn. Magn. Mater.* **84** 157
[16] Bauer E, Gratz G, Pillmayer N, Häufler T, Lees M, Gignoux D and Schmitt D 1990 *Physica* B **163** 375
[17] Bauer E, Gignoux D, Schmitt D and Winzer K 1987 *J. Magn. Magn. Mater.* **69** 158
[18] Bauer E, Gratz E, Mikovits W, Sassik H and Kirchmayr H 1982 *J. Magn. Magn. Mater.* **29** 192
[19] Amato A and Sierro J 1985 *J. Magn. Magn. Mater.* **47/48** 526
[20] Gottwick U, Held R, Sparn G, Steglich F, Vey K, Assmus W, Rietschel H, Stewart G R and Giorgi A L 1987 *J. Magn. Magn. Mater.* **63/64** 341
[21] Bauer E, Gratz E, Hutflesz G and Müller H 1991 *J. Phys.: Condens. Matter* **3** 7641
[22] Bauer E, Gratz E, Hutflesz G, Bhattacharjee A K and Coqblin B 1992 *J. Magn. Magn. Mater.* **108** 159
[23] Grier B H, Lawrence J M, Horn S and Thompson J D 1988 *J. Phys. C: Solid State Phys.* **21** 1099
[24] Bhattacharjee A K, Coqblin B, Raki M, Forro L, Ayache C and Schmitt D 1989 *J. Physique* **50** 2781